ELASTO-PLASTIC DAMPER OPTIMIZATION ROUTINE FOR LATTICE TOWERS BASED ON GENERALIZED RESPONSE SPECTRUM ANALYSIS

Yuki Terazawa[1], Toru Takeuchi[2]

[1]Ph. D candidate, Department of Architecture and Building Engineering, Tokyo Institute of Technology, 158-8550, Japan
terazawa.y.aa@m.titech.ac.jp
[2]Professor, Department of Architecture and Building Engineering, Tokyo Institute of Technology, 158-8550, Japan
takeuchi.t.ab@m.titech.ac.jp

Editor's Note: The first author of this paper is one of the four winners of the 2018 Hangai Prize, awarded for outstanding papers that are submitted for presentation and publication at the annual IASS Symposium by younger members of the Association (under 30 years old). It is re-published here with permission of the editors of the proceedings of the IASS Symposium 2018: "Creativity in Structural Design" held in July 2018 in Boston, USA.

DOI: Digital Object Identifier to be provided by Editor when assigned upon publication

ABSTRACT

This paper presents a damper design routine for highly indeterminate 3-D structures utilizing computational optimization and response spectrum analysis, which has been extended to incorporate non-proportional damping. This enables a more efficient design process than trial-and-error approaches. An example retrofit of a seismically deficient lattice tower using buckling-restrained braces is presented.

Keywords: *response spectrum analysis, complex stiffness, structural optimization, elasto-plastic damper, lattice tower.*

1. INTRODUCTION

Numerous spatial structures have been seriously damaged in recent earthquakes, as shown in Fig. 1. As these structures often support key infrastructure or are designated as post-disaster shelters, enhanced seismic performance is required. An efficient retrofit technique is to replace some members with elasto-plastic dampers, such as buckling-restrained braces (BRBs), which act as fuses (Ookouchi et al. [1]).

The challenge is to determine a set of discrete locations where a limited number of dampers would be most effective. While this task is well suited to computational optimization, the complicated vibration characteristics pose a challenge to most existing procedures. Thus, in practice, designers tend to rely on time-consuming trial-and-error studies using non-linear response history analysis (NLRHA). In contrast, conventional multistory buildings are commonly designed using the faster response spectrum analysis (RSA) with equivalent linearization approaches (JSSI [2]). However, these are generally limited to isolated and framed buildings systems that are easily translated into lumped mass models and have a predominate mode. With a suitable RSA method, computational optimization of damped spatial structures is a promising design strategy to develop creative structural designs, particularly given recent trends towards the use of algorithmic modelling, scripting and cloud-based high performance computing servers.

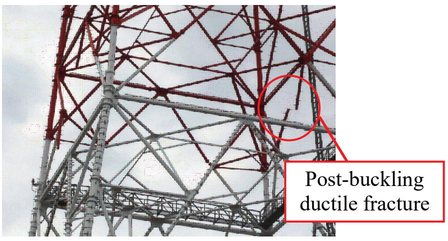

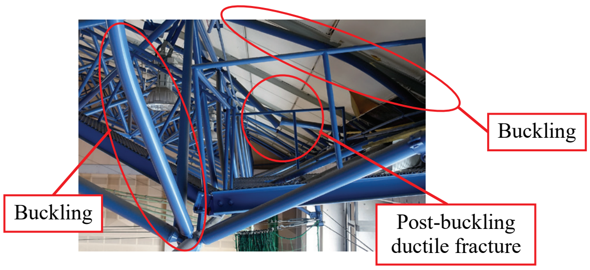

Figure 1: *(a) Lattice tower in 2007 Chuetsu-oki earthquake, (b) Double layer grid in 2016 Kumamoto earthquake*

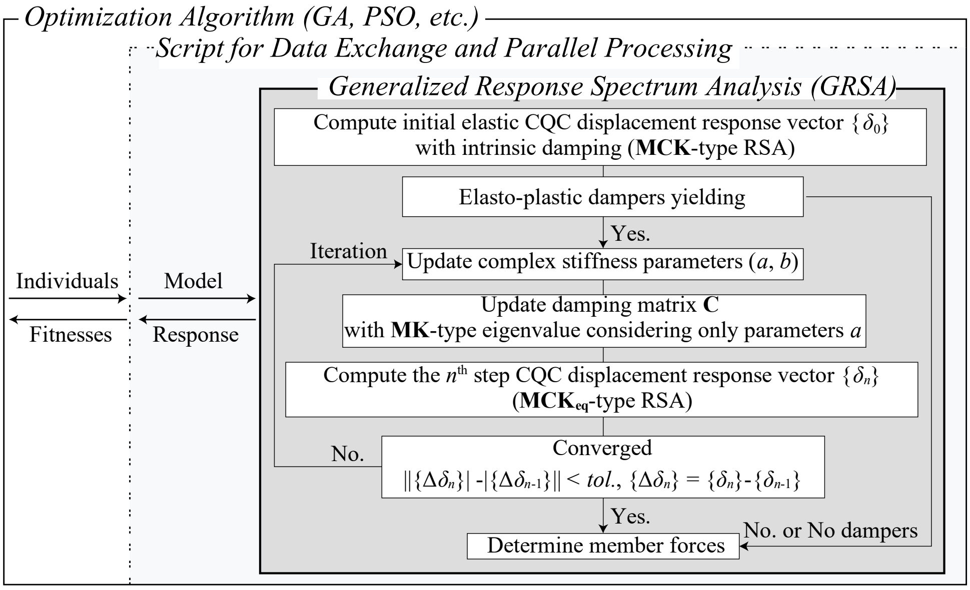

Figure 2: *Optimization routine based on GRSA*

Table 1: *Equivalent linear parameters for complex stiffness matrix, based on a bilinear hysteresis*

Method Series	a	b	ξ'	Ref.
Peak damping method (PDM)	$\{1+p(\mu-1)\}/\mu$	$(\pi/4)(1-p)(\mu-1)/\mu^2$	$b/(2a)$	[6]
Average damping method (ADM)	$\{1+p(\mu-1)\}/\mu$	$2a\xi'$	Integral average value PDM-ξ' by μ	[7]

This paper proposes a RSA-based optimization design routine permitting discretely placed elasto-plastic dampers in 3-D models. This procedure is applied to the retrofit of an existing lattice tower, comparing the efficiency of an existing damper layout and sizing to the computationally generated schemes.

2. PROPOSED COMPUTATIONAL ROUTINE

The proposed routine is outlined in Fig. 2, where complex eigenvalue analysis and RSA are iteratively applied, a process referred to as "Generalized Response Spectrum Analysis" (GRSA, Terazawa et al. [3]). In this figure, the non-damped, real symmetrically damped and complex asymmetrically damped systems are denoted "**MK**," "**MCK**," and "**MCK**$_{\mathbf{eq}}$," respectively. The complex stiffness $\mathbf{K}_{\mathbf{eq}}$ accounts for amplitude-dependent equivalent damping due to yielding, and is accommodated in a proposed extension of the complete quadratic combination (CQC) method. Since the seismic response evaluation step dominates the analysis time and constitutes the novel contribution of this paper, the optimization algorithm itself is only briefly described.

2.1. Complex Stiffness for Elasto-plastic Damper Braces

Complex stiffness (Myclestad [4]) is suitable for simulating amplitude-dependency, as compared to the equivalent viscoelasticity representation of elasto-plasticity, which results in higher modal damping ratios due to frequency-dependent damping. So that the 3-D models may also be used for NLRHA, a complex element stiffness matrix K_{eq} was developed for elasto-plastic dampers based on a space truss element, but as the axial terms are of primary interest to this paper, only these are included in Eq. 1.

$$K_{eq} = \left(\begin{array}{cc|cc} (a+ib\,\mathrm{sgn}\,\omega_e)k_x & \cdots & -(a+ib\,\mathrm{sgn}\,\omega_e)k_x & \cdots \\ \vdots & \ddots & \vdots & \ddots \\ \hline -(a+ib\,\mathrm{sgn}\,\omega_e)k_x & \cdots & (a+ib\,\mathrm{sgn}\,\omega_e)k_x & \cdots \\ \vdots & \ddots & \vdots & \ddots \end{array} \right) + K_G \quad (1)$$

where k_x is the axial stiffness, K_G is the geometric stiffness matrix, a is a stiffness coefficient, b is a damping coefficient and ω_e is the circular excitation frequency. The local coordinate system is aligned with the x-axis corresponding to the longitudinal member axis, and the member is assumed prismatic.

As argued in well-known studies (e.g. Jacobsen [6] and Newmark et al. [7]), the equivalent linear method for elasto-plasticity can have any type, due to its amplitude-dependency. In this study, two parameter formulations subjected to bilinear-type hysteresis are compared in Table 1, with μ the ductility ratio, p the post yield stiffness ratio and ξ' the element damping ratio. The parameters are iteratively updated based on the CQC responses, until convergence with the assumed ductility μ is achieved.

2.2. Response Evaluation for Complex Asymmetric Damped Systems

Complex eigenvalue analysis enables the exact computation of modal damping ratios and mode shapes for damped systems. Although the conventional RSA is unavailable for non-classical damped systems, Sinha and Igusa [5] proposed the modified CQC (Eq. (2)) based on the established conjugate property of **MCK** systems. This paper extends this method to **MCK$_{eq}$** systems, which have a complex stiffness term.

$$ {}_iR_{\mathrm{CQC}} = \sqrt{\sum_{s=1}^{n}\sum_{r=1}^{n} {}_iB_s\, {}_iB_r\, S_{d_s}(\omega_s,\xi_s)\, S_{d_r}(\omega_r,\xi_r)\cos({}_i\theta_s - {}_i\theta_r)\rho_{sr}} \quad (2) $$

where i is the i^{th} degree of freedom, s and r are mode numbers, ρ is the mode correlation coefficient for the conventional CQC method, ω is the modal circular frequency, ξ is the modal damping ratio, $S_d\,(\omega,\,\xi)$ is the spectral displacement, λ is the complex eigenvalue, β is the complex participation factor, ϕ is the complex eigenvector, "*" refers to the conjugate property, B is the real valued participation vector ($B = 2|\mathrm{Re}(\lambda^*\beta\phi)/\sin(\theta)|$) and θ is the approximate phase angle ($\theta = \tan^{-1}(-\mathrm{Re}(\lambda^*\beta\phi)/\mathrm{Re}(\beta\phi))$).

The characteristic equation for the **MCK$_{eq}$** system is shown in Eq. (3) and Eq. (4), with the eigenvalue distribution from the example structure (introduced later) illustrated in Fig. 3. Complex stiffness is a fictional expression and some eigenvalues produce infinite oscillations. However, by employing the signum function, it is easy to extract modal groups for the **MK$_{eq}$** system due to symmetry. In contrast, the axes of symmetry in the **MCK$_{eq}$** system are dependent on the viscous damping ξ_v of each mode, and some eigenvalues (related to infinite oscillations in **MK$_{eq}$**) shift to quadrants corresponding to damped oscillations. This lack of symmetry would normally make it impossible to directly extract the modal parameters (ξ_v, ξ_k, ω_0). Nevertheless, the true damped oscillations may still be obtained by identifying appropriate conjugate pairs, for example the pair given by the first and third lines in Eq. (4). This conjugate property is an essential feature of the modified CQC method, and permits modal responses of the **MCK$_{eq}$** system to be determined from a conventional **MCK** elastic response spectra, with natural circular frequencies given by $\omega = |\lambda|$, and modal damping ratios by $\xi = -\mathrm{Re}(\lambda)/\omega$.

$$ \lambda^2 + 2\xi_v\omega_0\lambda + (a + ib\ \mathrm{sgn}\omega_e)\omega_0^2 = 0 \quad (3) $$

$$ \lambda = \begin{cases} \begin{cases} -(\xi_v+\xi_k)\omega_0 + i\sqrt{(a-\xi_v^2)+\xi_k^2}\,\omega_0 \\ -(\xi_v-\xi_k)\omega_0 - i\sqrt{(a-\xi_v^2)+\xi_k^2}\,\omega_0 \end{cases} & (\omega_e > 0) \\ \begin{cases} -(\xi_v+\xi_k)\omega_0 - i\sqrt{(a-\xi_v^2)+\xi_k^2}\,\omega_0 \\ -(\xi_v-\xi_k)\omega_0 + i\sqrt{(a-\xi_v^2)+\xi_k^2}\,\omega_0 \end{cases} & (\omega_e < 0) \end{cases}, $$

$$ \xi_k = \sqrt{\{-(a-\xi_v^2) + \sqrt{(a-\xi_v^2)^2 + b^2}\}/2} \quad (4) $$

where ω_0 is the non-damped circular frequency, ξ_v is the damping ratio (related only to viscous damping), ξ_k is the damping ratio related to both the viscous damping and complex stiffness.

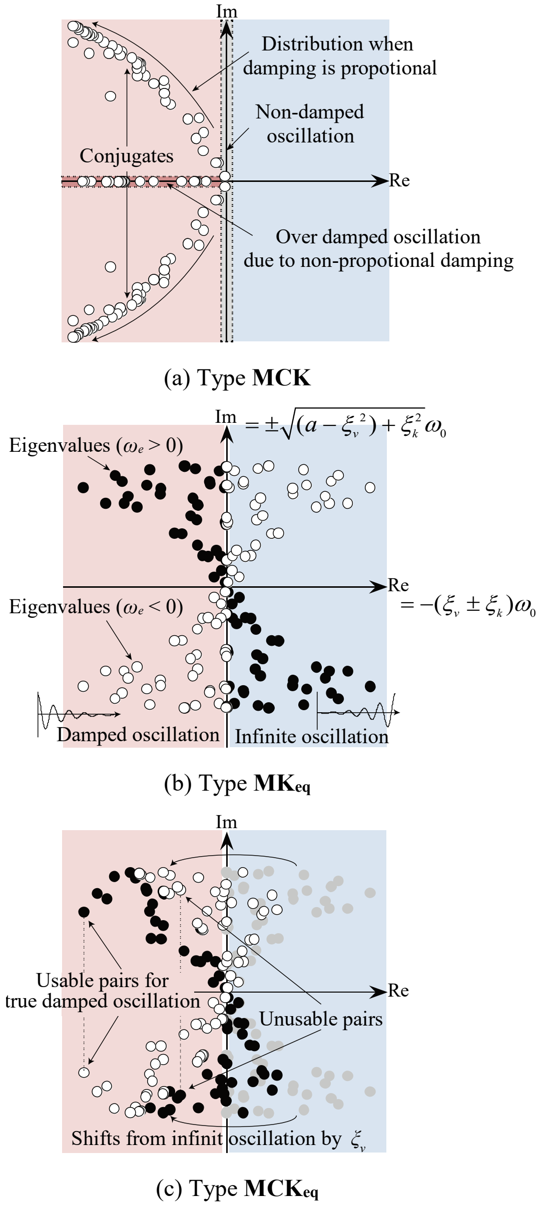

Figure 3: *Complex eigenvalues for damped systems with complex stiffness or additional viscoelasticity*

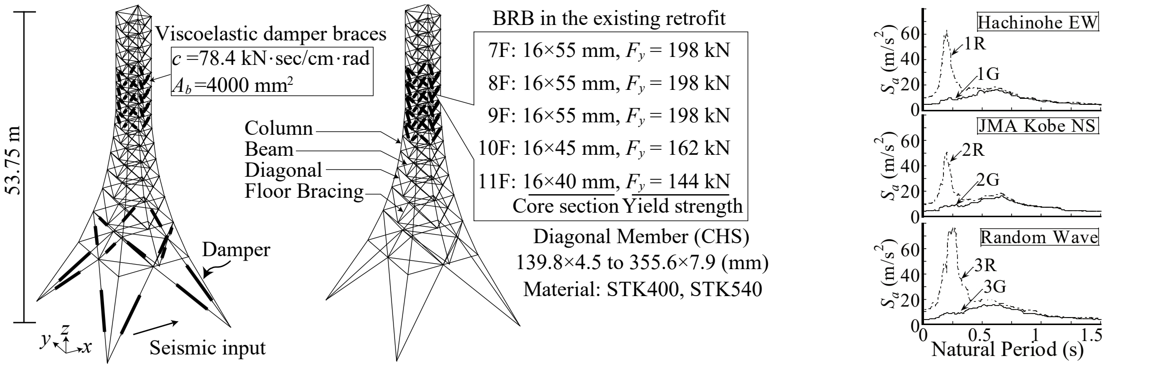

(a) VE Model (b) EP Model (c) Response Spectra ($\xi = 0.05$)

Figure 4: *Lattice tower model and spectrally matched ground motions*

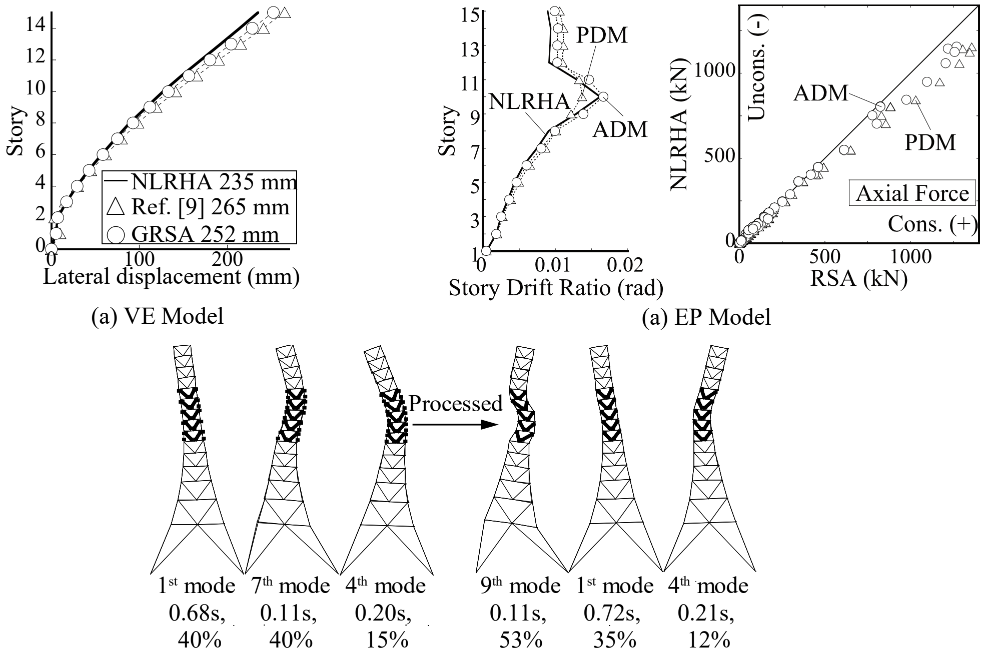

(a) VE Model (a) EP Model

(c) Dominant mode shifts in EP-ADM

Figure 5: *Comparison of GRSA and NLRHA results*

The complex eigenvalues are computed according to Foss [8], with convergence determined from the computed displacements, as indicated in Fig. 2. For the examples in this paper, convergence was obtained within 10 iterations. The acceleration and corresponding pseudo displacement response spectra were prepared in advance for a range of damping ratios (ξ_0 = 0.01, 0.02, 0.03, 0.05, 0.1, 0.15, 0.20, and 0.30) and the response reduction due to damping determined from $D_h=\sqrt{(1+25\xi_0)/(1+25\xi)}$ ([2]).

An implicit solution (Newmark beta method) was used for Non-linear response history analysis (NLRHA), including geometric and material nonlinearities. Although the GRSA routine uses the initial model coordinates, local coordinates (related to the rotation matrix and the stiffness distribution in the global matrix) were adjusted step-by-step using an updated Lagrangian incremental formulation in the NLRHA. This is a common limitation of modal response analysis methods, including GRSA.

3. TARGET LATTICE TOWER AND VALIDATION EXAMPLES

To validate the proposed GRSA method, the existing lattice telecommunication tower shown in Fig. 4 was analyzed. This tower was constructed in Japan, and was recently retrofitted with buckling-restrained braces (BRBs) [1], which is treated as elasto-plastic dampers in this paper. The BRB layout and sizes used in the existing retrofit are shown in the Fig. 4(b) EP model. The core material is a low yield strength Japanese steel LY225 (p = 0.02). Additionally, a retrofit employing viscoelastic dampers (VE model) was also prepared to confirm the improvement from the previous proposal [9], which adopted a conventional equivalent linear approach for simple, multi-degree of freedom systems [2]. A suite of 3 records (1G: Hachinohe EW, 2G: JMA Kobe NS and 3G: site-specific artificial random wave) were spectrally matched to the Japanese Level 2 design spectrum (Fig. 4(c)). As the lattice tower is situated at the top of a building (26m), the amplified response at the roof level was also developed (waves 1R to 3R). Sufficient modes to achieve a mass ratio of at least 90% were selected and 1% intrinsic damping adopted, reflecting the bare welded steel construction and height. The mass ratio is calculated as follows.

$$M_s = 2 \times \{1\}^{\mathrm{T}} \mathbf{M} \,\mathrm{Re}\left(\lambda_s \beta_s \{\phi_s\}\right) \tag{3}$$

As indicated by Fig. 5, the GRSA method has excellent agreement with the non-linear response history analysis results, and compares favorably to the previous method [9] used for the VE model. As indicated in Fig. 5(c), higher modes have significant contributions to the response of the EP model. Therefore, the average damping method (ADM) [6] parameter formulation has slightly better accuracy, as the member damping ratio *ξ'* is averaged over the contributing modes. Hence, ADM was used in the following chapters. It should be noted that other structures with a single predominate mode studied as part of this research found the peak damping method [6] to be more accurate, though this is outside the scope of this paper.

The computational resources required for the non-linear response history analysis are substantial, as the analysis model features 810 degrees-of-freedom. For the EP model, each non-linear response history analysis run took 15 to 30 min to complete, while the GRSA method took just 5 to 10s running on a local desktop computer equipped with one Intel Core i7 (3.6 GHz), which indicates that the GRSA is computationally efficient. With the exception of some numerical libraries, the entire source code was written by the first author.

4. ELASTO-PLASTIC DAMPER OPTIMIZATION

The proposed computational optimization damper design routine is demonstrated for the lattice tower retrofit, comparing the effectiveness of the as-built damper layout and distribution to the optimized results. Note that the existing retrofit as shown in Fig. 4(b) employed a trial and error approach using non-linear response history analysis with the primary objective of preventing member buckling.

Target objectives for the optimization are indicated in Table 2. A simple Genetic Algorithm was adopted for the layout optimization, and in a sequential step, Particle Swarm Optimization used to determine the damper distribution. For the layout optimization step, the number of BRB dampers was constrained to be similar to the existing retrofit and the yield strengths fixed as 388 kN (1F and 2F), and 200 kN (3F to 15F). For the distribution step, all diagonal members for a given retrofit story were required to be the same size and limited to 140 to 250 kN to ensure sufficient strength under wind load demands. For each optimization step, either the Story Drift Ratio (SDR) or Demand Capacity Ratio (DCR) was minimized, the later calculated as the member buckling utilization. Fitness was determined as the average value of the absolute maximum component of the response vector over the suite of ground or roof level waves, with the former representing an optimization of the tower placed directly on the ground. Optimization parameters are detailed in Table 3.

One cluster node of a campus supercomputer (TSUBAME3.0 at Tokyo Institute of Technology)

Table 2: *Optimization problem matrix*

Optimize	Damper Layout (Fixed Size)		Damper Distribution (Fixed Layout)	
Algorithm	Simple Genetic Algoritm		Particle Swarm Optimization	
Minimize	Ave. Max. SDRs	Ave. Max. DCRs	Ave. Max. SDRs	Ave. Max. DCRs
Subject to	$\Sigma x_i = 5$	$\Sigma x_i = 5$	$140 \leqq x_i \leqq 250$	$140 \leqq x_i \leqq 250$
Response to	1G to 3G	1G to 3G	1G to 3G	1G to 3G
	1R to 3R	1R to 3R	1R to 3R	1R to 3R

Table 3: *Optimization algorithm specifications*

Simple Genetic Algoritm			Particle Swarm Optimization			
Selection	Crossing	Mutation	Inertia	Personal Best Priority	Global Best Priority	Particles
Tournament (3 inds.)	Uniform (60%)	Shuffle Index (1%)	1.0	2.0	2.0	100

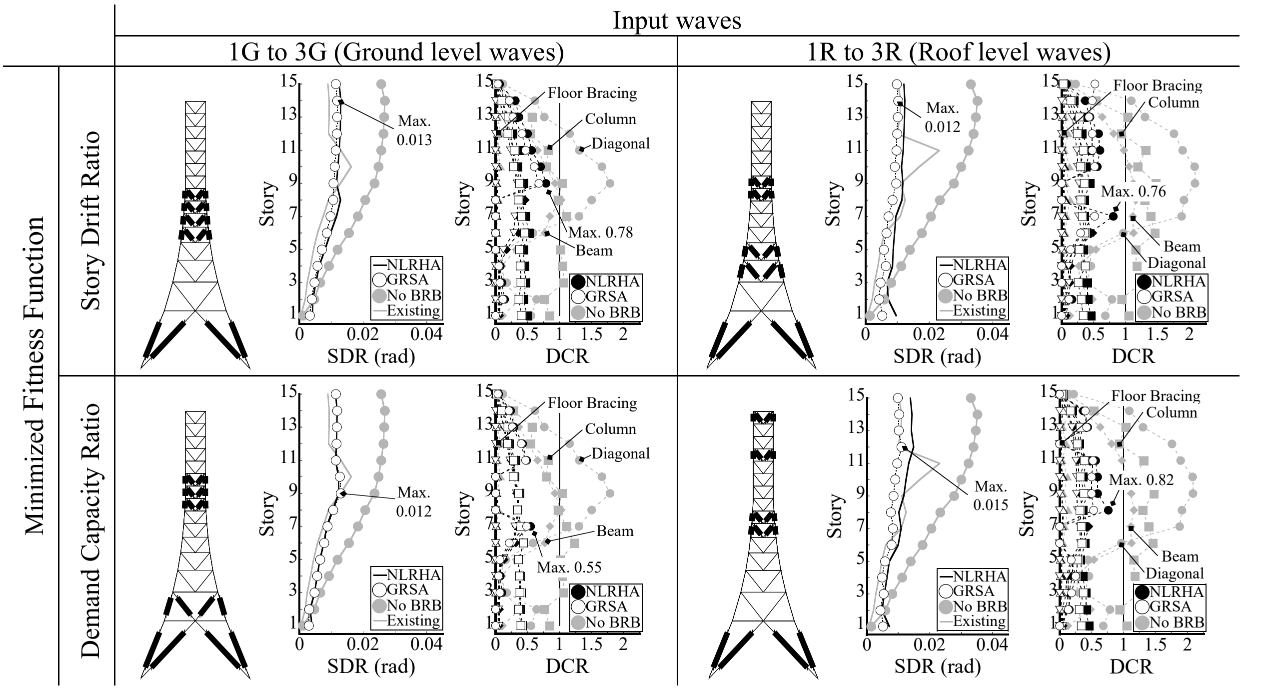

Figure 6: *Damper layout optimization results (BRBs are arranged in 1F to 15F., ex. Responses to 1G and 1R)*

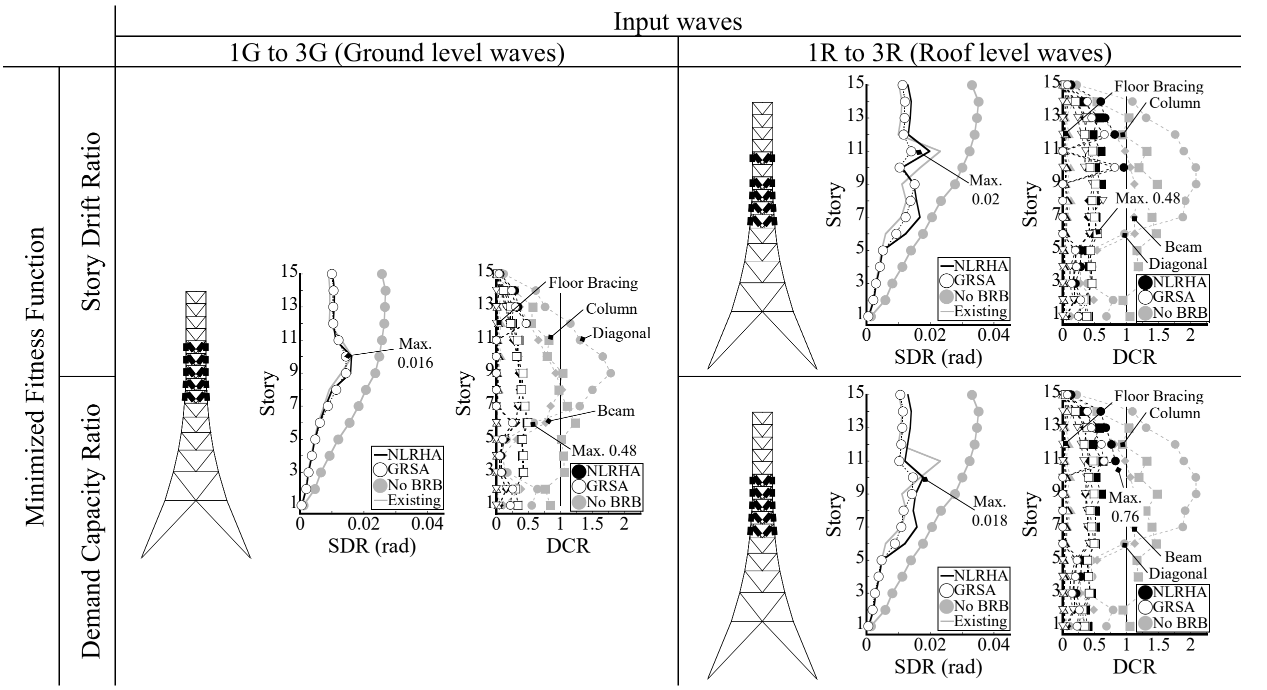

Figure 7: *Damper layout optimization results (BRBs are arranged in 3F to 15F., ex. Responses to 1G and 1R)*

was used instead of running the optimization on a cloud server. Python scripts were developed to distribute the parallel processing jobs, control the optimization algorithms (DEAP 1.1.0) and to pre- and post-process the results for the GRSA procedure. The computation time took approximately 30 min for the layout optimization, and 2 hr. for the distribution optimization, a marked improvement when compared to the trial-and-error studies using non-linear response history analysis.

4.1. Layout Optimization with Simple Genetic Algorithm

Optimal layouts for each suite of ground motions (ground vs roof level) and target objective (story drift vs buckling utilization) are shown in Fig. 6 and Fig.

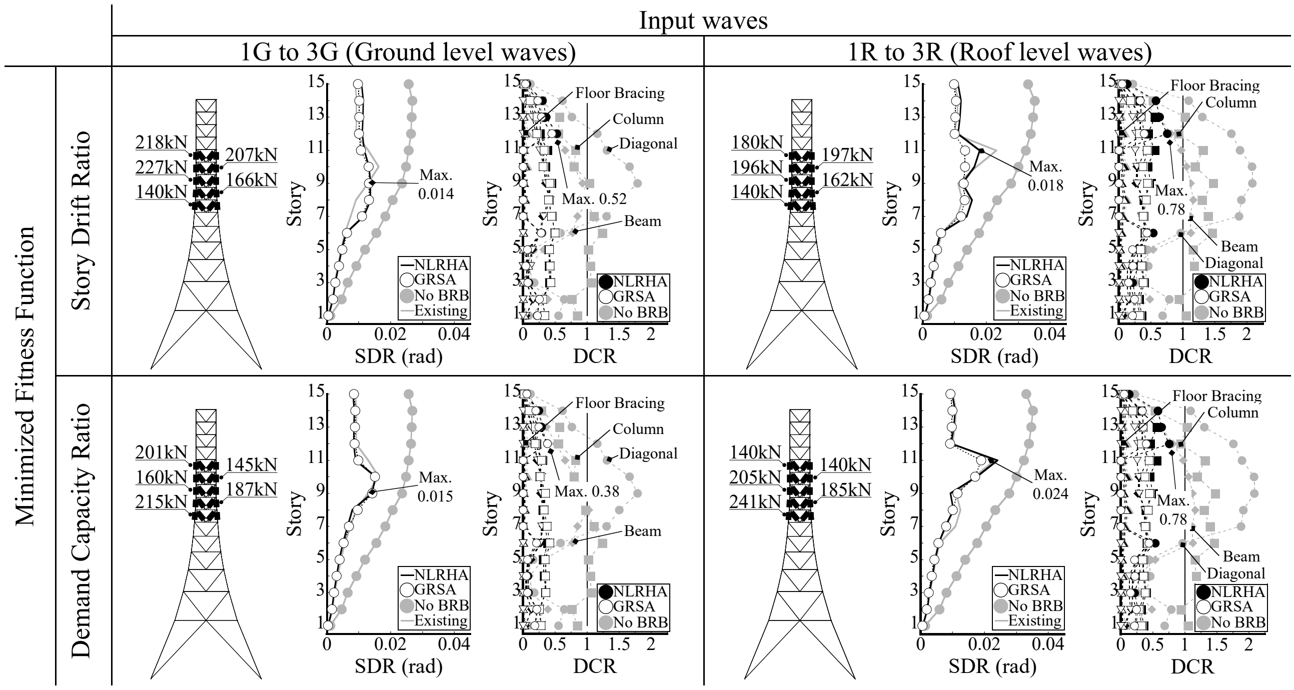

Figure 8: *Damper distribution optimization results (ex. Responses to 1G and 1R)*

7. In Fig. 6, BRBs at the lowest level are permitted, similar to a typical damper design strategy [2] and the previous VE damper study [9]. While a first story damper is usually the most effective and is selected for each optimal design, this tower would require a small, but exceptionally long (~10m) damper, which poses buildability challenges. The difference in layout amongst the upper stories can be attributed to the simplistic strategy adopted in the original design, where diagonal members that buckle in NLRHA are directly replaced until a satisfactory response is obtained. This approach apparently does not necessarily lead to the most efficient overall design. In Fig. 7, the first story brace was left non-retrofitted, with BRBs only permitted on for tiers 6F to 11F. Under this constraint, the existing layout amongst the upper stories happened to be the optimum solution for both objective functions, particularly for the suite of ground level waves.

4.2. Distribution Optimization with Particle Swarm Optimization

As the layout optimization from Fig. 7 is relatively stable and consistent with the implemented layout, distribution optimization was applied just for this configuration, with the results listed in Table 4 and response shown in Fig. 8. There is a clear difference when optimizing for each target criteria, with larger dampers concentrated into the upper stories to minimize story drift, but into the lower stories to minimize the buckling utilization factor (DCR). While the actual BRB sizes differ, the design optimized for buckling utilization corresponds with the general distribution of the implemented solution. Hence, the engineer's design concept for this particular lattice tower retrofit proved reasonably good in "preventing member buckling as much as possible." Nevertheless, several good alternative design options and trends are generated by the computational approach, which may not have been otherwise realized. It should be noted however that while the layout and distribution trends are usefully indicated by the optimal solutions, the results are dependent on the input waves, suggesting that there may be no absolute optimum solution to every possible scenario. As a final note, the GRSA results have good agreement for practical use in Fig. 6 to Fig. 8 with the non-linear response history analysis results, confirming the accuracy and effectiveness of the proposed method.

Table 4: *Damper distribution optimization results*

Minimize	Response to	Damper Size (kN)				
		7F	8F	9F	10F	11F
Ave. Max. SDRs	1G to 3G	140	166	227	207	218
	1R to 3R	140	162	196	197	180
Ave. Max. DCRs	1G to 3G	215	187	160	145	201
	1R to 3R	241	185	205	140	140
Existing Retrofit		198	198	198	162	144

5. CONCLUSION

This paper proposes a damper optimization design routine based on the Generalized Response Spectrum Analysis (GRSA) derived from the modified CQC and complex stiffness methods. The proposed analysis method may be used for direct response spectrum analysis of 3-D structural analysis models including dampers of various types, with buckling-restrained braces used in this study. As response spectrum analysis requires relatively few computational resources, this makes the proposed method ideal for genetic optimization studies, offering an alternative to trial-and-error based approaches. The author is planning to distribute the optimization routine as an open source module or a component for future work.

An existing lattice telecommunication retrofit where members are replaced with buckling-restrained braces was studied to illustrate the computational design process. While improved layouts and distributions were identified for certain constraint and target objectives, the existing design was found to be close to the optimal solution for minimizing the buckling utilization. As the optimal result depends on the selected seismic waves, this should be used as a tool to help explore the design space, rather than as a black box solution. Nevertheless, the accuracy of the proposed method compares favorably with non-linear response history analysis.

The energy-dissipation devices discussed in this study are limited to linear viscous, linear viscoelastic, or elasto-plastic dampers. Using equivalent linear approaches for the frequency-dependent damping and an alternative element as “Voigt model,” GRSA can be applied to nonlinear viscous or nonlinear viscoelastic dampers, both assumed to be included in the phase updating the damping matrix, as shown Fig. 2.

ACKNOWLEDGMENTS

The first author would like to thank Dr. Matsui for providing the photograph of the damaged lattice tower and Mr. Sitler for the proofreading. This work was supported by a Grant-in-Aid from the Japan Society for the Promotion of Science Fellowships (No. 16J04303).

REFERENCES

[1] Y. Ookouchi, T. Takeuchi, T. Uchiyama, K. Suzuki, T. Sugiyama, T. Ogawa and S. Kato "Experimental studies of tower structures with hysteretic dampers," *Proc. IASS 2005, IASS 2005 symposium*, Bucharest, Romania, pp. 299-306, 2005.

[2] Japan Society of Seismic Isolation (JSSI), *Manual for Design and Construction of Passively-Controlled Buildings 3rd Edition*, Daioh Co., Ltd, 2013. (In Japanese)

[3] Y. Terazawa and T. Takeuchi, “Generalized Response Spectrum Analysis for Structures with Dampers,” Earthquake Spectra, accessed 2018. 5. 31, DOI: https://doi.org/10.1193/092217EQS188M

[4] N. O. Myclestad, "The concept of complex damping," *J. Appl. Mech.*, Vol. 19, pp. 284-286, 1952.

[5] R. Sinha and T. Igusa, "CQC and SRSS methods for non-classically damped structures," *Earth. Eng. & Struct Dyn.*, Vol. 24, pp. 615-619, 1995.

[6] L. S. Jacobsen, "Damping in composite structure," *Proc. 2WCEE, WCEE 1960*, Tokyo, Japan, pp. 1029-1043, 1960.

[7] N. M. Newmark and E. Rosenblueth, “Chapter 11” in *Fundamental of Earthquake Engineering*, Prentice-Hall, 1971.

[8] K. A. Foss, "Coordinates which uncouple the equation of motion of damped linear dynamic systems," *J. Appl. Mech.*, Vol. 32, pp. 361-364, 1958.

[9] T. Takeuchi, Y. Kinouchi, R. Matsui and T. Ogawa, "Optimal arrangement of energy-dissipating members for seismic retrofitting of truss structures," *Am. J. Eng. & Appl. Sci.*, Vol. 8, pp. 455-464. 2015.